Cooperative Interactions between the Two DNA Binding Domains of Pax3: Helix 2 of the Paired Domain Is in the Proximity of the Amino Terminus of the Homeodomain

Sergio Apuzzo and Philippe Gros*

Department of Biochemistry, McGill University, Montreal, Canada

Received October 10, 2006; Revised Manuscript Received January 17, 2007

ABSTRACT: Pax3 is a transcription factor that plays an important role during neurogenesis and myogenesis, and Pax3 mutant animals display neural tube defects and lack limb muscles. Pax3 harbors two DNA binding domains, the paired domain (PD) and a paired-type homeodomain (HD). Genetic and biochemical data have (i) identified strong cooperative interactions between the PD and HD domains for DNA binding in the intact Pax3 protein and (ii) suggested an important role for the amino-terminal portions of both domains in such cooperativity. We have studied proximity relationships between the PD and HD of Pax3. For this, we have used a cross-linking strategy with the bifunctional thiol reagent bismaleimidoethane (BMOE) in 21 mutants bearing pairs of cysteine residues (DCM) inserted in strategic locations of a functional Pax3 protein otherwise devoid of endogenous cysteine residues. All 21 DCMs were characterized for protein stability, for DNA binding by the PD and HD, and for the effect of BMOE on protein binding to PD, HD, or PD−HD combined DNA targets. BMOE-induced cross-links in DCMs were detected as slower migrating species on immunoblots. Mutants bearing double cysteine insertions (I59C/S222C, S73C/Q219C, and V78C/K218C) showed the most robust cross-linking upon BMOE exposure. These cross-linking studies suggest that portions of helix 1 (I59), helix 2 (S73), and the loop between helices 2 and 3 (V78) of the PD are in the proximity of the N-terminal segment of the HD (K218, Q219, and S222) in the tertiary structure of Pax3. These results are compatible with a model in which the PD and HD are organized in an everted arrangement, with the N-terminal portion of the PD being in the proximity of the N-terminus of the HD. This arrangement may be important for the noted PD−HD cooperativity in DNA binding.

Pax3 is a member of the Pax family, a group of transcription factors that play critical roles during mammalian development (*1*−*12*). Pax3 is expressed in a number of embryonic structures (somites, the neural tube, and several neural crest cell-derived lineages) and is essential for the normal process of myogenesis and neurogenesis (*13*, *14*). A mutation in the mouse *Pax3* gene causes severe neural tube defects (spina bifida and exencephaly) and the absence of limb musculature; likewise, in humans, mutations in *PAX*3 cause Waardenburg syndrome (WS), a condition associated with sensorineural deafness, craniofacial abnormalities, and pigmentary disturbances (*13*, *15*−*21*). Pax3 appears to orchestrate the expression of a number of target genes during normal development, but aberrant *PAX*3 activity causes alveolar rhabdomyosarcoma (*22*, *23*). Structurally, Pax proteins are defined by the presence of a unique DNA binding domain called the paired domain (PD).[1] In addition, Pax3 and several other Pax proteins contain a second DNA binding domain, a paired-type homeodomain (HD) (*2*, *24*). Other structural domains of Pax proteins include a conserved octapeptide (OP) in the segment linking the PD and HD and the proline-, serine-, and threonine-rich (PST) transactivation domain at the carboxyl terminus.

High-resolution three-dimensional structures (*25*, *26*) show that the PD is formed by N-terminal (PAI) and C-terminal (RED) subdomains, each consisting of a three-helix fold that includes a helix−turn−helix (HTH) motif, with the C-terminal helix of each HTH making base-specific contacts in the major groove of DNA (*25*, *26*). The linker joining the PAI and RED subdomains also makes base-specific contacts in the minor groove of DNA. In addition to the HTH motif, the PAI subdomain harbors a β-turn structure at its amino terminus that also makes critical contacts in the minor groove of DNA (*25*, *26*). The DNA sequences recognized by the PD can be bound by both subdomains (class I sequences) or only by the PAI subdomain (class II sequences) (*27*, *28*). The structure of the DNA-bound Prd paired-type HD shows three α-helices, with the two most C-terminal forming a HTH motif (*29*−*32*). The C-terminal helix of the HTH makes base-specific contacts in the major groove of DNA and is responsible for DNA binding specificity. The N-terminal segment preceding the HTH motif makes additional contacts in the minor groove of DNA. A unique feature of pt-HDs is their ability to dimerize on palindromic sequences of the type TAAT(N_{2-3})ATTA (*30*−*32*).

* To whom correspondence should be addressed: Department of Biochemistry, McGill University, 3655 Sir William Osler Promenade, room 907, Montreal, QC, Canada H3G-1Y6. Phone: (514) 398-7291. Fax: (514) 398-2603. E-mail: philippe.gros@mcgill.ca.

[1] Abbreviations: PD, paired domain; HD, homeodomain; HTH, helix−turn−helix; SCM, single-cysteine mutant; DCM, double-cysteine mutant; BMOE, bismaleimidoethane.

10.1021/bi062107q CCC: $37.00
Published on Web 02/27/2007

Table 1: Oligonucleotides Used for Pax3 Mutagenesis

substitution	mutagenic primer (5′ to 3′)[a]
I59C	ATCCGCCACAAG***TGT***GTGGAGATGGCC
S73C	CCGAGCGTCATTT***G***TCGCCAGCTTCGC
V78C	CGCCAGCTTCGC***TGT***TCCCATGGATCC
L215C	CCTGATTTACCG***TGT***AAGAGGAAGCAGCGCCGATCGAGAACCACCTTC
K216C	GATTTACCGCTG***TGT***AGGAAGCAGCGCAGGTCTAGAACCACCTTC
R217C	GACTCTGAACCAGATCTACCGCTGAAG***T***G***T***AAGCAGCGCAGGTCGCGAACCACCTTC
K218C	CCGCTGAAGAGG***TGT***CAGCGCAGGTCGCGAACCACCTTC
Q219C	GATGAAGGATCCGATATTGACTCTGAACCTGATTTACCGCTGAAGAGGAAG***TGT***CGCAGGAGC
S222C	CAGCGCAGG***T***GCCGTACGACCTTCACG
T225C	GAGCAGAACC***TG***CTTCACGGCAGAGCAGCTGGAGGAACTGGAGCGCGCGTTCGAGAG

[a] Nucleotide substitutions leading to amino acid changes are in bold and italicized, and those that introduce silent restriction sites are underlined.

Although the PD and HD can bind to cognate DNA sequences when expressed individually, a large body of genetic and biochemical data indicates that the two domains are functionally interdependent in intact Pax3. For instance, the G42R mutation in the PD of Pax3 from the *Splotch-delayed* (*Sp*^{d}) mouse mutant abrogates DNA binding by the PD but also impairs DNA binding by the HD. Interestingly, deleting helix 2 of the PAI subdomain in the context of the G42R mutation (*Sp*^{d}) restores DNA binding by the HD, suggesting that this helix is involved in cooperative interaction between the PD and HD of Pax3 (*33*). Studies in chimeric Pax3 proteins have shown that the PD can modulate both the DNA binding specificity and dimerization potential of heterologous HDs (*34*). Conversely, studies of the HD mutation R53G found in a Waardenburg patient show that it impairs DNA binding by both the HD and the PD (*35*). Site-specific modification of single-cysteine Pax3 mutants with thiol reagents has shown that independent modification of position 82 in the PD and position 263 in the HD (V263C) abrogates DNA binding by both the PD and HD (*36*). Finally, protease sensitivity studies in Pax3 mutants bearing engineered Factor Xa sites either in the linker separating the PAI and RED motif (position 100) or upstream of the HD (position 216) revealed that DNA binding by either the PD or the HD causes a structural change in the other DNA binding domain (*37*), providing a structural basis for the observed interdependence of DNA binding. Additional studies with single-cysteine mutants independently introduced into the second α-helix (α2, positions 59−80) and in the *β*-hairpin (positions 40−41) at the amino terminus of the PD identified a number of positions (Q40, I59, V60, P69, S70, I72, S73, L76, V78, and S79C) at which NEM modification abrogated DNA binding by the PD and HD (*38*). Three-dimensional modeling revealed that these residues are not randomly distributed but rather cluster in a hydrophobic pocket, representing a possible docking site for the HD during DNA binding by the intact protein (*38*).

The objective of this study was to characterize further the structural basis of the HD−PD functional interaction in Pax3 and possibly identify individual residues of the HD that may come into the proximity of the PD during DNA binding. Proximity relationships were investigated in Pax3 mutants bearing pairs of single cysteines inserted at different positions of the amino terminus of the PD and of the HD [double-cysteine mutants (DCMs)], followed by cross-linking with the thiol-specific bifunctional reagent BMOE. For this, we created 21 Pax3 mutants bearing pairs of cysteines between positions 59, 73, and 78 in the amino terminus of the PD on one hand and seven positions (215−219, 222, and 225) in the amino terminus of the HD on the other hand. The ability of BMOE to induce cross-linking of Cys pairs in Pax3 mutants bound to different DNA targets recognized by either the PD (P3OPT), the HD (P2), or both (PH0) was evaluated. These cross-linking studies suggest that portions of the PD, α1 (I59), α2 (S73), and the loop joining α2 and α3 (V78), are approximately 8 Å from the N-terminus of the HD (K218, Q219, and S222) in the tertiary structure of Pax3 (*39*).

MATERIALS AND METHODS

Mutagenesis. The construction of the pMT2 expression plasmid containing the entire coding region of wild-type (WT) *Pax3* cDNA has been described previously (*33*, *36*). *Pax3* was modified by the in-frame addition of c-Myc and HA epitopes at the N- and C-termini, respectively, thereby generating the pMT2/Myc-Pax3-HA WT construct (*37*). The construction and functional characterization of a Pax3 mutant lacking cysteines [Cys-less (CL)] have been described previously (*36*), and this CL Pax3 was similarly modified by insertion of epitopes to create pMT2/Myc-Pax3-HA CL. The generation of the three PD (CL/I59C, CL/S73C, and CL/V78C) single-cysteine mutants used in this study was previously described (*38*). The seven other single-cysteine mutants have cysteines introduced into the N-terminal arm and upstream linker of the HD (CL/L215C, CL/K216C, CL/R217C, CL/K218C, CL/Q219C, CL/S222C, and CL/T225C) by PCR mutagenesis using the pMT2/Myc-Pax3-HA CL as a template with the primers listed in Table 1. Pax3 contains a *Kpn*I cassette defined by two endogenous *Kpn*I restriction sites at positions 563 and 1500. Swapping of *Kpn*I cassettes of linker−HD SCM constructs into the three PD SCM constructs permitted the generation of the following 21 double-cysteine mutants: I59C/L215C, I59C/K216C, I59C/R217C, I59C/K218C, I59C/Q219C, I59C/S222C, I59C/T225C, S73C/L215C, S73C/K216C, S73C/R217C, S73C/K218C, S73C/Q219C, S73C/S222C, S73C/T225C, V78C/L215C, V78C/K216C, V78C/R217C, V78C/K218C, V78C/Q219C, V78C/S222C, and V78C/T225C. Each mutation was verified by nucleotide sequencing, and the accessibility of restriction sites for cloning was verified by endonuclease fragmentation.

Expression and Detection of Pax3 Mutants. The expression plasmids were used to transiently transfect COS-7 monkey cells. One million cells were plated in Dulbecco's modified Eagle's medium containing 10% fetal bovine serum and were transfected by the calcium phosphate coprecipitation method using 15 μg of plasmid DNA doubly purified by ultracentrifugation on cesium chloride density gradients. Calcium−

DNA precipitates were placed onto the cells for 5 h and then treated with HBS [0.14 M NaCl, 5 mM KCl, 0.75 mM Na_2HPO_4, 6 mM dextrose, and 25 mM HEPES (pH 7.05)] containing 15% glycerol for 1 min. The cells were then washed and placed in complete Dulbecco's modified Eagle's medium. Whole cell extracts were prepared 24 h following glycerol shock by sonication in a buffer containing 20 mM HEPES (pH 7.6), 0.15 M NaCl, 0.5 mM tris(2-carboxyethyl)phosphine hydrochloride (TCEP), 0.2 mM EDTA, 0.2 mM EGTA, and a mixture of protease inhibitors: aprotinin, pepstatin, and leupeptin used at 1 mg/mL and phenylmethanesulfonyl fluoride used at 1 mM. These extracts were stored frozen at −70 °C until they were used. To assess Pax3 mutant protein expression and stability, aliquots of whole cell extracts were analyzed by electrophoresis on acrylamide-containing SDS gels (SDS−PAGE), followed by electrotransfer onto nitrocellulose membranes and immunoblotting. Immunodetection was performed with mouse monoclonal anti-HA antibody (BabCO, Berkeley, CA) at a dilution of 1:1000 and visualized by enhanced chemiluminescence using a sheep anti-mouse horseradish peroxidase-conjugated secondary antibody (Amersham Biosciences). Subsequently, the immunoblots were submerged in stripping buffer [100 mM 2-mercaptoethanool, 2% SDS, and 62.5 mM Tris-HCl (pH 6.7)] for 30 min at 50 °C and washed with TBST buffer [10 mM Tris-HCl (pH 8), 150 mM NaCl, and 0.1% Tween 20 at 20 °C] at room temperature. The membranes were then probed with mouse monoclonal anti-Myc antibody (BabCO) at a dilution of 1:1000 and visualized by enhanced chemiluminescence using a sheep anti-mouse horseradish peroxidase-conjugated secondary antibody (Amersham Biosciences).

Electrophoretic Mobility Shift Assays. Electrophoretic mobility shift assays (EMSA) were performed as previously described (*36*). Each protein−DNA binding reaction was carried out using approximately 8 μg of total cell extracts from transiently transfected COS-7 monkey cells and 10 fmol (0.06 μCi) of radioactively labeled double-stranded oligonucleotides corresponding to different Pax3 target sequences. The final concentration of labeled oligonucleotide in the binding reaction mixture is 0.5 nM. Whole cell extracts were incubated with ^{32}P-labeled probes in a volume of 20 μL containing 10 mM Tris-HCl (pH 7.5), 50 mM KCl, 1 mM TCEP, 2 mM spermidine, 2 mg/mL BSA, and 10% glycerol. To reduce the level of nonspecific binding, 1 μg of poly(dI-dC) was included in binding studies with PD-specific probes and composite probes with both PD and HD sites, while 2 μg of heat-inactivated salmon sperm DNA was added to binding reaction mixtures involving HD-specific probes. Following a 30 min incubation at room temperature, samples were electrophoresed at 12 V/cm in 6% acrylamide/bisacrylamide (29:1) gels containing 0.25× or 0.5× TBE [1× TBE is 0.18 M Tris-HCl, 0.18 M boric acid, and 4 mM EDTA (pH 8.3)]. Gels were dried under vacuum and exposed to Kodak BMS film with an intensifying screen. PD-specific sequences P6CON [5′-TGGAATTCAGGAAAAATTTTCACGCTTGAGTTCACAGCTCGAGTA-3′ (*28*)] and P3OPT [5′-TGGTGGTCACGCCTCATTGAATATTA-3′ (*39*, *40*)], HD-specific sequence P2 [5′-GATCCTGAGTCTAATTGATTACTGTACAGG-3′ (*31*)], and the composite PD−HD binding site PH0 [5′-GATTTCTTCCAATTAGTCACGCTTGAGTG-3′ (*41*)] were synthesized as complementary oligonucleotide pairs with recessed 3′ ends for end labeling with [α-^{32}P]dATP (3000 Ci/mmol; NEN) using the Klenow fragment of DNA polymerase.

The thiol-specific reagent *N*-ethylmaleimide (NEM, Pierce) was prepared as a 32 mM stock solution in water. Bismaleimidoethane (BMOE), a sulfhydryl-to-sulfhydryl cross-linking reagent (Molecular Probes) was prepared as a 32 mM stock solution in 100% dimethyl sulfoxide. To assess the effect of NEM or BMOE on DNA binding, they were added as a 0.5 μL aliquot to a 4 μL volume of whole cell extract (final concentration of 3.55 mM), followed by a 30 min incubation at room temperature prior to the addition of the ^{32}P-labeled probe and EMSA. Western blotting was carried out with whole cell extracts treated with non-radiolabeled DNA prior to BMOE treatment to assess the extent of cross-linking in double-cysteine mutants. When BMOE-treated whole cell extracts were destined for Western blotting, they were treated with NEM (3.55 mM, 30 min at 20 °C) prior to SDS−PAGE to block any remaining unmodified cysteines and to prevent nonspecific cross-linking. Films generated from Western blotting were used to perform densitometry studies to quantify the amount of chemiluminescence using a Fuji LAS-1000 instrument, as we have previously described (*36*, *37*).

RESULTS

Construction of Pax3 Mutants Bearing Single- or Double-Cysteine Insertions. A large body of biochemical and genetic data indicates that DNA binding by Pax3 involves cooperative interactions between the PD and the HD. Indeed, point mutations (*35*) or site-specific modifications of single cysteines in either the PD or the HD abrogate DNA binding by both domains (*36*), and DNA binding by either the PD or the HD causes a structural change in the other domain (*37*). In addition, a number of studies have suggested that this functional cooperation may involve physical interactions between the two domains. The goal of our study was to investigate proximity relationships between the PD and HD, including the identification of specific residues mapping at the interface of such interactions. We targeted the amino-terminal portions of both the PD and the HD as two sites that are most likely to physically interact in intact Pax3. This was based on the following published data. DNA binding studies with the *Drosophila* Prd protein using hybrid DNA sequences (PH0) optimized for combined PD and HD binding show that the two domains are everted (*41*). Additional modeling studies suggest that the N-terminus of the PAI subdomain is closely apposed to the N-terminus of the HD when bound to the combined PH0 site (*41*), with helix 2 of the PAI domain very close of the N-terminal extension of the HD. A critical role of PAI subdomain helix 2 in the interaction with the HD is supported by functional studies showing that deletion of helix 2 in the context of the *Sp*^{d} mutant allele of Pax3 (G42R) restores DNA binding by the HD in the context of the mutant protein (*34*). Finally, studies in Pax3−Phox chimeras suggest that the C-terminal portion of the linker domain separating the PD and HD contributes to functional interactions between the two domains in DNA binding (*34*).

Here, we investigated proximity relationships in the Pax3 protein by cross-linking. For this, we used a Pax3 mutant that is devoid of cysteine (CL) residues but that retains wild-

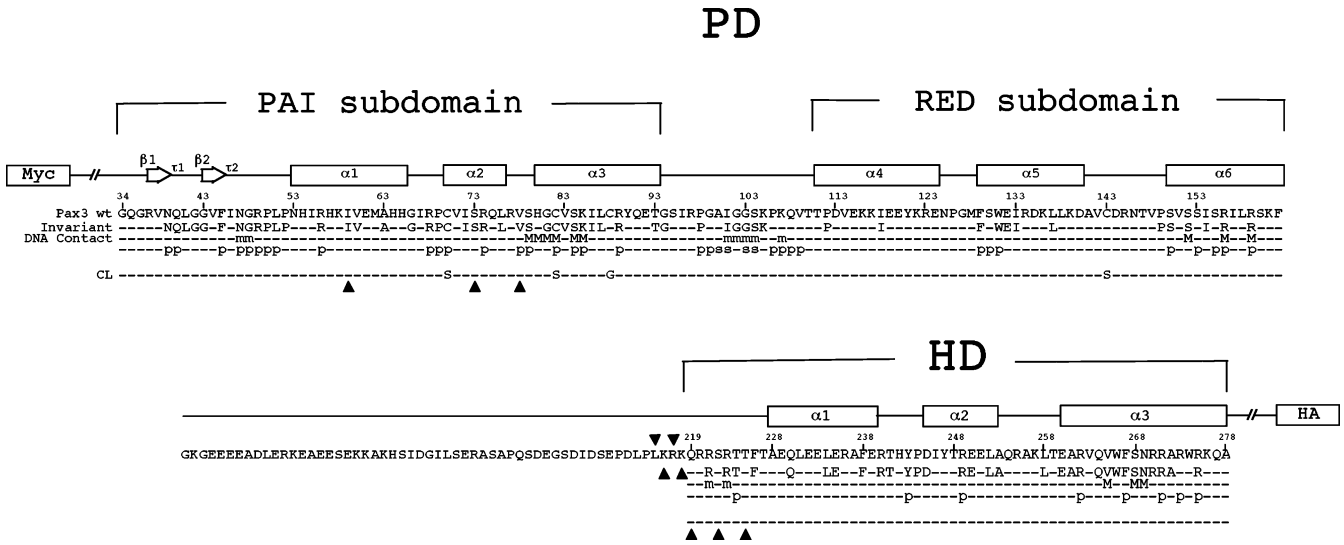

FIGURE 1: Site-directed mutagenesis of the PD of Pax3. The amino acid sequence for positions 34−278 of Pax3 is shown, including a schematic representation of the N-terminal (PAI) and C-terminal (RED) subdomains of the PD, together with structural features based on the three-dimensional structure of the PD of the Pax6 protein (*β*, *β*-strand; *τ*, *β*-turn; α, α-helix) (*25*). Invariant residues among all known PDs are identified below the schematic representation. The type of predicted DNA contacts made by these residues (p, phosphate; m, minor groove; M, major groove) is shown. The positions and nature of the mutations introduced into Pax3 to create the Cys-less (CL) mutant are given. Residues targeted when generating single-cysteine mutants are denoted with filled arrowheads. The figure also includes a schematic representation of the Pax3 linker and homeodomain (HD), including the presence and position of predicted structural features, invariant amino acid residues, and the number and types of DNA contacts (as for the PD). The positions of the c-Myc and hemagglutinin (HA) epitope tags inserted in-frame at the amino and carboxyl termini of Pax3, respectively, are shown.

type DNA binding properties with respect to PD or HD target sequences (*36*, *38*). We created double-cysteine mutants (DCM) bearing one cysteine in individual positions of the PD and the HD; the proximity of the two cysteines was assessed by the ability of a bifunctional, thiol-specific cross-linking agent (BMOE) to make a covalent adduct between the two targeted positions. The effect of DNA binding by the PD and the HD on the formation of such adducts was also investigated. The implementation of this strategy requires that both inserted Cys residues be at exposed positions accessible to the sulfhydryl reagent. For this, we selected positions at which Cys insertion does not affect DNA binding but yet confer *N*-ethylmaleimide (NEM) modification sensitivity of DNA binding in the context of a single-Cys mutant. Such single-Cys mutants were then systematically reconstructed as DCM and functionally analyzed.

Previous cysteine scanning mutagenesis identified a hydrophobic pocket in the N-terminal segment of the PAI subdomain at which insertion of a single Cys confers NEM sensitivity to DNA binding by the PD and HD in the intact protein (*38*). In this proposed docking site for the HD, positions I59 (α-helix 1), S73 (α-helix 2), and V78 (α2−α3 linker) of the PAI subdomain (Figure 1) were most sensitive to NEM treatment and were selected for potential PD candidates for the current cross-linking studies. In the HD, the N-terminal arm (first nine residues) was targeted for study. In preliminary experiments, substitution of each of these nine residues with cysteine in SCM showed that only three positions (Q219, S222, and T225) could tolerate this replacement without a loss of DNA binding by the HD (data not shown). These, together with four adjacent residues from the linker domain (L215, K216, R217, and K218), were selected for potential HD candidates for cross-linking studies (Figure 1).

The following single-cysteine mutants (SCM) were created in the PD (CL/I59C, CL/S73C, and CL/V78C) and in the N-terminal part of the HD (CL/L215C, CL/K216C, CL/R217C, CL/K218C, CL/Q219C, CL/S222C, and CL/T225C) using the Pax3 CL backbone as a template. In addition, double-cysteine mutants (DCMs) were created by combining each of the three PD mutations with each of the seven HD mutations in a group of 21 DCMs.

Protein Expression and DNA Binding Properties of Pax3 Single- and Double-Cysteine Mutants. To facilitate detection of wild-type (WT), CL, and all SCMs and DCMs, cMyc and hemagglutinin (HA) epitope tags were inserted in-frame at the N-termini and C-termini of all constructs, respectively. All constructs were made using the pMT2 expression plasmid and were used to transiently transfect COS-7 monkey cells. Immunoblotting of whole cell extracts with either anti-HA or anti-c-Myc monoclonal antibodies shows that all SCMs and DCMs can be expressed at similar levels in COS-7 cells (Figure S1 of the Supporting Information). This indicates that none of the mutations had a major effect on the protein expression or stability in COS-7 cells. The effects of single- and double-cysteine substitutions on the DNA binding properties of the PD and the HD of Pax3 were assessed in each mutant by electrophoretic mobility shift assays (EMSAs). The DNA binding activity of the PD was measured using the PD-specific probes P3OPT (*39*, *40*) and P6CON (*28*) which have been shown to contain binding determinants for both the PAI and RED subdomains of the PD. The DNA binding activity of the homeodomain was determined using the P2 target sequence, which contains the TAAT(N_2)ATTA sequence previously shown to support cooperative dimerization of Pax3. Finally, all mutants were assessed for DNA binding activity with respect to the PD−HD composite site present in the PH0 probe. All SCMs and DCMs retained PD DNA binding activity for both the P3OPT and P6CON probes which was similar to that displayed by the WT or CL Pax3 protein (Figure 2). Most mutants retained DNA binding by the HD and showed dimerization on the

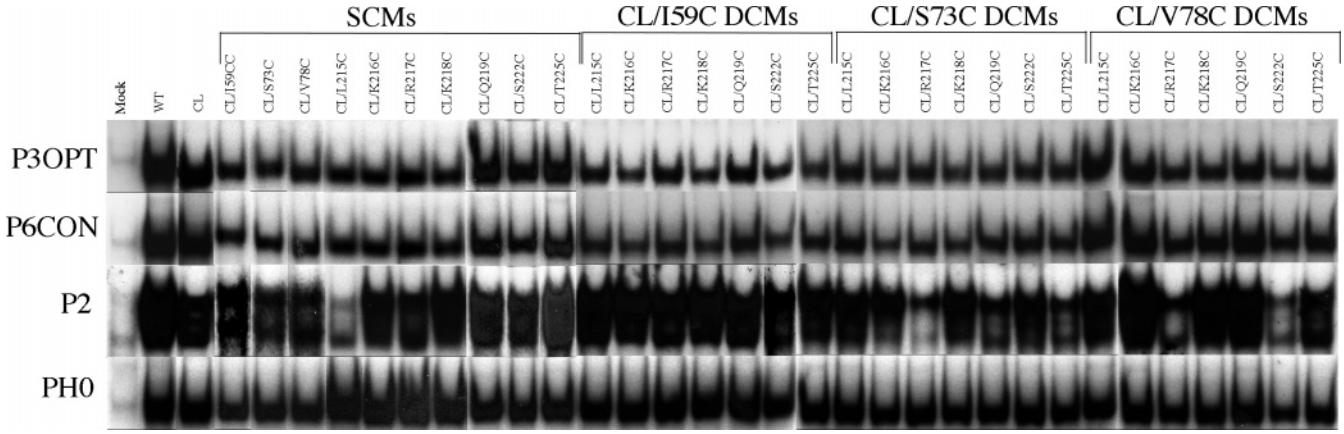

FIGURE 2: Paired domain and homeodomain DNA binding properties of the wild type, Pax3 CL, SCMs, and DCMs. Electrophoretic mobility shift assays were used to measure the DNA binding properties of Pax3 (WT), CL, SCMs, and DCMs against the paired domain (P3OPT and P6CON), the homeodomain (P2), and a paired domain−homeodomain composite site (PH0). Protein−DNA complexes were formed using total cell extracts from transiently transfected COS-7 cells and were resolved on 6% acrylamide nondenaturing gels, as described in Materials and Methods.

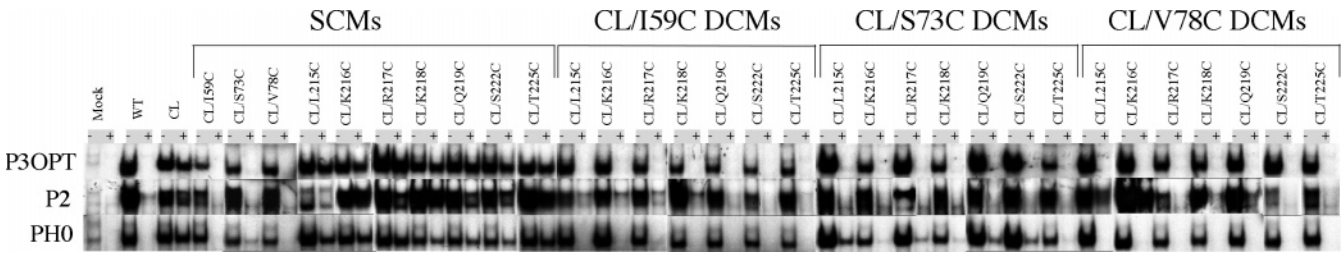

FIGURE 3: Effect of site-specific modifications on DNA binding properties of Pax3 mutants. Effects of bismaleimidoethane (BMOE) treatment on the paired domain and homeodomain DNA binding properties of the wild type (WT), CL, SCMs, and DCMs. Whole cell extracts from COS7 monkey cells (mock) or from cells expressing different Pax3 mutants were incubated with 0 (−) or 3.55 mM (+) BMOE prior to electrophoretic mobility shift assays. The DNA binding properties of the different Pax3 proteins were tested against the paired domain (P3OPT and P6CON), the homeodomain (P2), and a paired domain−homeodomain composite site (PH0).

P2 probe, with the possible exception of SCM CL/L215C and the DCMs S73C/R217C and V78C/S222C that exhibited a decreased level of binding to this target. However, all mutants exhibited wild-type binding activity for the composite probe PH0 (Figure 2). These results indicate that most of the mutations either alone or in combination have no effect on DNA binding by Pax3, and none appear to alter the ability of the protein to bind a PD−HD composite site.

Effect of Thiol-Specific Reagents on DNA Binding by Single- and Double-Cysteine Mutants. Both *N*-ethylmaleimide (NEM) and bismaleimidoethane (BMOE) can covalently modify and alkylate cysteine residues and were used for site-specific modification of SCMs and DCMs. BMOE contains two maleimide functional groups, as opposed to one with NEM, and thus can create covalent adducts (cross-links) between cysteines showing the spatial proximity in an otherwise intact protein. The effect of monofunctional NEM (Figure S2 of the Supporting Information) and bifunctional BMOE (Figure 3) on DNA binding properties of WT, CL, and SCMs and DCMs was evaluated by EMSA, using PD (P3OPT), HD (P2), and combined PD−HD (PH0) target sequences. Whole cell extracts from COS-7 cells expressing CL or SCMs or DCMs were incubated with either 3.55 mM NEM or 3.55 mM BMOE prior to the DNA binding properties being tested via an EMSA. For control WT Pax3, treatment with either NEM or BMOE abrogates DNA binding by the PD and HD for both the individual and the combined target sequence. On the other hand, DNA binding by the Pax3 CL control protein to all probes tested was completely insensitive to NEM and BMOE treatment (Figure S2 of the Supporting Information Figure 3).

The effect of NEM (Figure S2 of the Supporting Information) or BMOE treatment (Figure 3) on the DNA binding properties of SCMs and DCMs was identical for each mutant, and only results obtained with BMOE will be reviewed. As previously reported for NEM (*38*), alkylation of PD positions 59 (I59C), 73 (S73C), and 78 (V78C) by the BMOE reagent abrogated DNA binding by the PD and HD in the corresponding SCM (Figure 3). This formally verifies that sulfhydryl groups introduced at these positions are accessible to the bifunctional BMOE reagent. Modification of single cysteines inserted at any of the seven positions of the N-terminal portion of the HD was without consequences on DNA binding of corresponding SCMs to the P3OPT probe. On the other hand, BMOE modification of the L215C, R217C, Q219C, and S222C SCM mutants had some effect on DNA binding of the HD to the P2 probe. Nevertheless, BMOE treatment had no effect on binding to the PD−HD composite site in any of the seven HD SCMs that were tested (Figure 3).

As expected from the observed BMOE sensitivity of DNA binding by the single mutants I59C, S73C, and V78C, all DCMs exhibited BMOE sensitivity for all probes that were tested. DCMs V78C/L215C and V78C/K216C were notable exceptions; although both showed BMOE sensitive DNA binding to PD and PD−HD probes, they showed partial (V78C/L215C) or complete (V78C/K216C) insensitivity for binding to the P2 probe.

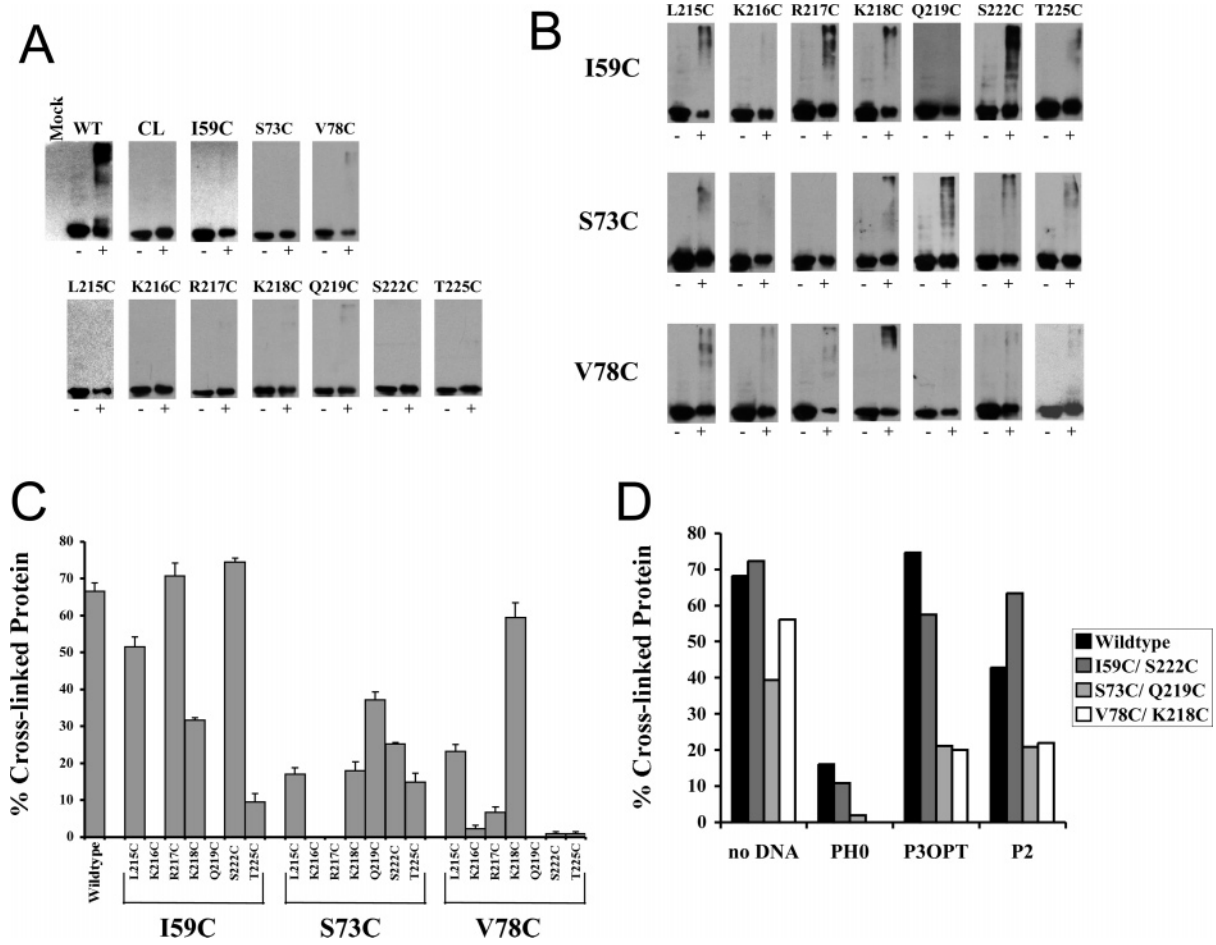

FIGURE 4: Detection and quantification of cross-linking species of Pax3 mutants. Fifteen micrograms of whole cell extracts from COS-7 cells transfected with either the wild type (WT), CL, or the different single-cysteine mutants (A) or double-cysteine mutants (B) was incubated with 3.55 mM BMOE, and the mixture was analyzed via SDS−PAGE on 12% acrylamide gels and immunoblotting with an anti-HA antibody. Cross-linked species are visible as higher-molecular mass bands. (C) The immunoblots of non-DNA-bound, BMOE-exposed double-cysteine mutants probed with the anti-HA antibody were scanned by densitometry, and the percentage of cross-linked protein was determined. (D) The immunoblots of BMOE-exposed wild-type Pax3 and selected DCMs probed with the anti-HA antibody were scanned by densitometry, and the percentage of cross-linked protein was determined with and without prior incubation of a PD-specific probe (P3OPT), a HD-specific probe (P2), and a composite PD−HD probe (PH0).

Cross-Linking Studies in SCMs and DCMs. Proximity relationships between pairs of cysteines were studied by cross-linking in DCMs. In these experiments, WT, CL, and all SCMs and DCMs were treated with BMOE and cross-linked species were detected by SDS−PAGE and immunoblotting with monoclonal anti-HA (Figure 4) or anti-cMyc antibody (data not shown). In these experiments, cross-linked Pax3 proteins are detected as higher-molecular mass species of slower electrophoretic mobility on denaturing, detergent-containing (SDS) polyacrylamide gels (*42*). Exposure of WT Pax3 to BMOE followed by SDS−PAGE and immunoblotting results in the appearance of cross-linked Pax3 species of slower mobility that are absent from the control untreated sample (Figure 4A). Such cross-links probably arise from the reaction of BMOE with two or more of the seven endogenous cysteines present in the WT protein. In agreement with this proposal, no such cross-links are detected when the CL mutant is similarly treated with BMOE. These results additionally show that under our experimental conditions, the BMOE reagent can induce the formation of cysteine-specific cross-links. Treatment of all 10 SCMs with BMOE does not result in the formation of slowly migrating cross-links. This absence of cross-links in BMOE-treated SCMs together with the demonstrated accessibility of at least single-Cys insertions at positions 59, 73, and 78 of the PD (Figure 3) strongly suggests that BMOE does not induce the formation of intermolecular cross-links in these SCMs. Exposure of DCMs to BMOE resulted in the appearance of cross-links for some of the combinations that were tested (Figure 4B,C). This, together with the absence of such cross-links in all 10 similarly treated SCMs (Figure 4B,C), strongly suggests that these BMOE-induced cross-links in DCMs are specific for the individual cysteine pairs and occur in an intramolecular fashion.

Studies in DCMs with a PD cysteine at position 59 indicated that this residue could react with all N-terminal HD positions with the exception of K216C and Q219C, with the most robust cross-link formed between I59C and S222C (Figure 4B,C). To confirm that the detected cross-links were indeed intramolecular (as opposed to intermolecular), SCMs I59C and S222C were mixed together, treated with BMOE, and analyzed by SDS−PAGE and immunoblotting. No cross-links were observed under such conditions, confirming that the noted reactivity between I59C and S222C was indeed intramolecular (data not shown). A cysteine at position 73 of the PD (S73C) could react with five of the seven

N-terminal HD cysteine insertions, with the strongest reactivity detected for Q219C. Finally, V78C cross-linked primarily with K218C and particularly L215C but showed little if any reactivity with any of the other positions.

In summary, of the seven cysteines inserted into the N-terminal position of the HD, only L215C and K218C form cross-linked species with all three targeted positions in the PD. Also, only K216C fails to significantly cross-link with any of the PD cysteines that were tested. R217C appears to react only with PD positions 59 (I59C) and 78 (V78C), while Q219C reacts only with position 73 (S73C). Finally, HD cysteines S222C and T225C both only cross-link PD cysteines I59C and S73C (Figure 4B,C).

Effect of DNA Binding on BMOE-Induced Cross-Linking in DCMs. The effect of DNA binding by the PD and HD on proximity relationships in the Pax3 protein was further investigated by allowing DCMs to bind PD (P3OPT), HD (P2), or combined PD−HD targets (PH0) prior to treatment with BMOE and resolution of cross-linked products by SDS−PAGE and immunoblotting (Figure 4D and Figure S3 of the Supporting Information). For these studies, the amount of cross-linked species following BMOE treatment of WT and DCMs (in the absence of DNA) was first quantified by densitometry analysis of the immunoblots and is expressed as a percentage of the total detectable protein on the blot. The effect of DNA binding on the formation of cross-links in WT and DCMs was similarly quantified for each probe. We focused these studies on the four DCMs that exhibit the strongest BMOE-induced cross-linking between cysteines inserted into the PD and HD, namely, I59C/R217C, I59C/S222C, S73C/Q219C, and V78C/K218C (Figure 4D). Incubation of WT and DCM Pax3 variants with the combined PH0 sequence considerably reduced the degree of cross-linking induced by BMOE. Because the effect was seen with all proteins, we suspect that it may reflect a change in the overall accessibility of cysteine residues to the BMOE agent in the PH0-bound form of the protein. On the other hand, binding to PD- or HD-specific probes had both similar and distinct effects on BMOE-induced cross-linking in individual mutants. For example, in the I59C/S222C mutant, there was no effect of binding to P3OPT or P2 probes on BMOE-induced cross-links, while in the S73C/Q219C and V78C/K218C DCMs, binding to both probes caused a reduction in the level of cross-link formation. On the other hand, the I59C/R217C mutant had a distinct behavior, with significant inhibition of cross-linking when the PD engages in DNA binding and no effect when the protein binds DNA through the HD. These results suggest that DNA binding can induce local conformational changes in Pax3 that can be detected by quantitative changes in BMOE-induced cross-linking between individual cysteine pairs of unique DCM variants. In this case, such alterations most likely reflect DNA-induced changes in the distance or orientation of the two cysteines, as opposed to an overall change in the accessibility to the BMOE reagent.

DISCUSSION

We studied proximity relationships in the Pax3 protein by a cross-linking approach based on the use of a bifunctional sufhydryl cross-linker (BMOE) in Pax3 mutants bearing pairs of engineered cysteines. For this, discrete portions of the PD and HD previously shown to play a key role in cooperative interactions of the two domains for DNA binding were selected for cysteine insertion. In this approach, and to ascertain that cysteine mutagenesis did not affect the overall structure or function of the Pax3 protein, we purposely limited our study to positions at which replacement of the endogenous residue with cysteine was without consequences for DNA binding by the protein. The accessibility of individual Cys substitutions to alkylating agents was not determined directly but was inferred from the ability of NEM and BMOE to interfere with DNA binding by the targeted domain. In such an experimental scheme, BMOE insensitive Cys mutations may reflect (a) a lack of an effect of alkylation on DNA binding or (b) the inaccessibility of mutated positions to BMOE. The ability of BMOE to induce cross-links in a specific pair of double-cysteine mutants was also used as evidence that the two positions were accessible to reagent.

The three positions in the PD targeted for Cys mutagenesis (I59, S73, and V78) all exhibited BMOE sensitivity of DNA binding by the PD and the HD, confirming the accessibility of these three positions. The solvent accessibility of these three residues is in agreement with previous NEM sensitivity studies (*38*) and the noted capacity of cysteines at all three positions to form cross-links with a subset of cysteines introduced into the HD (Figure 4). On the other hand, none of the Cys mutations introduced into the N-terminal part of the HD showed BMOE sensitivity for DNA binding, except for small effects on HD DNA binding seen in mutants R217C, Q219C, S222C, and L215C. Therefore, it is likely that the BMOE sensitivity of DNA binding seen in all DCMs is caused in large part by the BMOE reactivity of Cys at the PD positions in these double mutants. On the other hand, the ability of all N-terminal HD Cys substitutions to form cross-links with one or several of the PD Cys insertions indicates that the HD cysteines were indeed accessible to the BMOE cross-linker. One exception is K216C, which failed to generate, upon BMOE exposure, robust cross-links with any of the three PD cysteines. In summary, DNA binding and cross-linking studies suggest that all PD and HD cysteines introduced into Pax3, with the possible exception of K216C, were accessible to BMOE and therefore may be solvent-exposed.

The BMOE-induced cross-links detected in WT Pax3 must arise from reaction of any two endogenous cysteines with the bifunctional cross-linker. The endogenous cysteines most likely to be BMOE-reactive are C70 in PAI helix 2, C82 in PAI helix 3, and C143 in the RED subdomain in the loop joining helices 5 and 6 (*43*). Indeed, mass spectroscopy experiments as well as mutagenesis studies have shown that under oxidative conditions a disulfide bridge is formed between Cys70 and Cys82 as well as between Cys82 and Cys143, thereby abrogating DNA binding via the PD. The lack of cross-links in Pax3 CL is indicative of the specificity of the BMOE reagent for cysteines, and the absence of cross-links in SCMs shows that any cross-links formed in DCMs are more likely the result of intramolecular cysteine cross-linking and not intermolecular cross-linking. In the DCMs that were analyzed, the most robust cross-links appeared to be formed between I59C and R217C, I59C and S222C, S73C and Q219C, and V78C and K218C. An obvious interpretation of these results is that these pairs of cysteines, and corre-

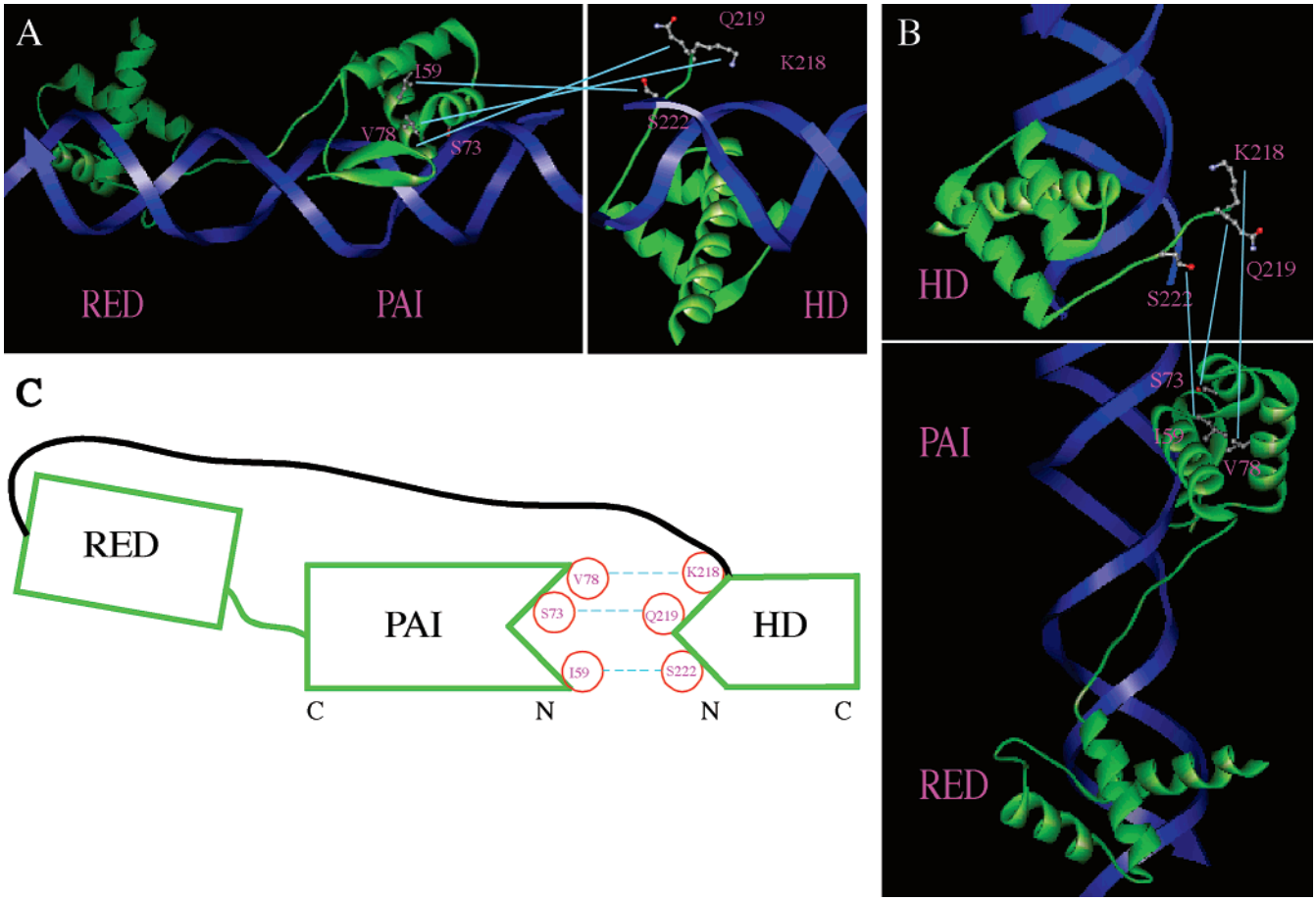

FIGURE 5: Structure of the DNA-bound paired domain and homeodomain. In panels A and B, the PAI and RED subdomains and the HD are shown on a three-dimensional DNA-bound structure (*25*, *32*). The three α-helices of each domain are shown, and the *β*-hairpin of the PAI subdomain is also displayed. The PD and HD are shown as a green ribbons drawn through the α-carbon backbone. The DNA strands are shown as blue ribbons through the sugar−phosphate backbone. The atoms of the side chains of residues targeted for cysteine substitution and at which BMOE modification causes cross-linking are shown (I59, S73, and V78 in the PD and K218, Q219, and S222 in the HD). In panels A and B, the PD and HD DNA-bound structures were used to construct a model of the two domains bound to a composite DNA sequence such as PH0, which contains both a PD and a HD DNA binding site that are juxtaposed (*41*). Panels A and B represent the front and rear views of the model, respectively. Panel C is a schematic model of the "head-to-head" orientation of the PD and HD that facilitates the PD−HD physical interaction responsible for the interdependence of DNA binding. The black line indicates the linker that joins the PD and HD. Turquoise lines in panels A−C link cysteine substitutions that undergo extensive cross-links when paired in a DCM exposed to BMOE.

sponding positions in the wild-type protein, are closest in space (~8 Å) among all the pairs that were tested (*51*). We believe that the slower migrating species detected by SDS−PAGE analysis of BMOE-treated double-cysteine mutants (Figure 4B) are intramolecular cross-linked DCMs. Although these slower migrating species may correspond to intermolecular cross-links between double-Cys Pax3 mutants and unrelated proteins present in transfected COS cell extracts (we are not working with purified proteins), such species are not detected when the two corresponding single-Cys mutants are mixed together prior to cross-linking (data not shown). This supports the contention that such higher-mobility species correspond to intramolecular as opposed to intermolecular cross-links in double-Cys mutants. In parallel studies of double-Cys MDR1 mutants by the same protocol, Clarke and his colleagues have indeed reported altered hydrodynamic properties of intramolecular cross-links in SDS−PAGE, including slower mobility (*42*).

The amount of BMOE-induced protein cross-links in WT and mutants was estimated by densitometry, and the effect of DNA binding by the PD and HD on the production of such cross-links was measured. Binding to the composite site sequence PH0 caused a dramatic decrease in the overall amount of BMOE-induced cross-linking in all proteins that were tested. One likely explanation of this observation is that DNA binding to PH0 increases the compactness and inflexibility of the protein and reduces the accessibility of cysteines to BMOE, hence decreasing the number of cross-links that are formed. It can be postulated that less cross-linking may occur simply because the PD moves closer to HD on PH0, but we believe that it is due to a conformational change in the protein. A decrease in the level of cross-linking may be ascribed to a number of possible conformational changes ranging from (a) a change from one rotamer to another of one or a few side chains of specific residues to (b) subtle local changes in conformation or (c) a dramatic rearrangement of the polypeptide backbone of the protein. We are in favor of the interpretation that a more dramatic conformational change occurs since it is in agreement with circular dichroism spectroscopy studies with the PD of Pax5 and Pax8 (*43*). These studies have shown that the PD adopts a more ordered structure with more helical content upon

DNA exposure (*43*). Also, X-ray crystallography and NMR studies of HD proteins have revealed an increased order of the HTH motif, including the N-terminal arm and the recognition helix, of the DNA-bound form of Pbx (*44*−*47*), Antennapedia (*48*), engrailed (*49*), and Oct-1 (*50*) proteins. Also, previous studies have shown that engineered protease sites in the PAI subdomain and N-terminal arm of the HD in Pax3 become less accessible to cleavage upon DNA exposure, indicating a more compact conformation of the DNA-bound form (*37*).

It has been established that for BMOE to induce cross-links, the two sulfhydryl side chains must be located 6−10.5 Å apart (average of 8 Å) (*51*). Therefore, one can conclude that the maximum intermolecular distances separating the above-mentioned pairs of residues must be within the range of 6−10.5 Å. The pairs of cysteines showing the most robust BMOE-induced cross-links (I59C and R217C, I59C and S222C, S73C and Q219C, and V78C and K218C) have been positioned on the three-dimensional structure of the DNA-bound models of the PD from Pax6 (*25*) and of the HD from *Drosophila* Prd (*32*) proteins. From this modeling, an everted positioning of the PD and HD for DNA binding to a combined site appears to be required to account for cross-linking results obtained here in DCMs variants. Such a model is in agreement with that previously proposed by Jun and Desplan for combined PD and HD binding of the *Drosophila* Prd protein to chimeric target sequences (*41*). The model suggests that the N-terminus of the PAI domain is closely apposed to the N-terminus of the HD when bound to the combined site. Their model suggests that the PD and HD bind opposite sides of the DNA helix with the N-terminal arm of the HD very close to helix 2 of the PAI subdomain. The PD−HD physical interaction suggested in this model may be responsible for the interdependence of DNA binding observed in Pax3 and may also be used to explain the interaction of the PD of Pax3 with the N-terminal arm of Msx1 (*52*). The model shown in Figure 5 indicates only the most extensive cross-linking patterns that have been observed. The most N-terminal I59 residue is closest to the most C-terminal residue of the N-terminal arm of the HD, S222C, while the most C-terminal PD residue V78 forms the most cross-links with and is closest to the most N-terminal HD residue K218. This is in accordance with the head-to-head orientation of the PD and HD when they are physically interacting. The cross-linking studies and the model proposed in Figure 5 support our previous study that implicates the role of residues I59, S73, and V78 in the formation of a hydrophobic pocket in the PD whereby the HD can dock and participate in the physical interaction responsible for DNA binding functional interdependence (*38*).

SUPPORTING INFORMATION AVAILABLE

Expression of Pax3 mutants in COS-7 monkey cells (Figure S1), the effect of site-specific modification on DNA binding properties of Pax3 mutants (Figure S2), and cross-linking species of Pax3 mutants that were incubated with DNA prior to BMOE exposure (Figure S3). This material is available free of charge via the Internet at http://pubs.acs.org.

REFERENCES

1. Bopp, D., Burri, M., Baumgartner, S., Frigerio, G., and Noll, M. (1986) Conservation of a large protein domain in the segmentation gene paired and in functionally related genes of *Drosophila*, *Cell 47*, 1033−1040.
2. Stuart, E. T., Kioussi, C., and Gruss, P. (1994) Mammalian Pax genes, *Annu. Rev. Genet. 28*, 219−236.
3. Balling, R., Deutsch, U., and Gruss, P. (1988) undulated, a mutation affecting the development of the mouse skeleton, has a point mutation in the paired box of Pax 1, *Cell 55*, 531−535.
4. Dahl, E., Koseki, H., and Balling, R. (1997) Pax genes and organogenesis, *BioEssays 19*, 755−765.
5. Glaser, T., Walton, D. S., and Maas, R. L. (1992) Genomic structure, evolutionary conservation and aniridia mutations in the human PAX6 gene, *Nat. Genet. 2*, 232−239.
6. Hill, R. E., Favor, J., Hogan, B. L., Ton, C. C., Saunders, G. F., Hanson, I. M., Prosser, J., Jordan, T., Hastie, N. D., and van Heyningen, V. (1991) Mouse small eye results from mutations in a paired-like homeobox-containing gene, *Nature 354*, 522−525.
7. Jordan, T., Hanson, I., Zaletayev, D., Hodgson, S., Prosser, J., Seawright, A., Hastie, N., and van Heyningen, V. (1992) The human PAX6 gene is mutated in two patients with aniridia, *Nat. Genet. 1*, 328−332.
8. Macchia, P. E., Lapi, P., Krude, H., Pirro, M. T., Missero, C., Chiovato, L., Souabni, A., Baserga, M., Tassi, V., Pinchera, A., Fenzi, G., Gruters, A., Busslinger, M., and Di Lauro, R. (1998) PAX8 mutations associated with congenital hypothyroidism caused by thyroid dysgenesis, *Nat. Genet. 19*, 83−86.
9. Mansouri, A., Chowdhury, K., and Gruss, P. (1998) Follicular cells of the thyroid gland require Pax8 gene function, *Nat. Genet. 19*, 87−90.
10. Sanyanusin, P., Schimmenti, L. A., McNoe, L. A., Ward, T. A., Pierpont, M. E., Sullivan, M. J., Dobyns, W. B., and Eccles, M. R. (1995) Mutation of the PAX2 gene in a family with optic nerve colobomas, renal anomalies and vesicoureteral reflux, *Nat. Genet. 9*, 358−364.
11. Sosa-Pineda, B., Chowdhury, K., Torres, M., Oliver, G., and Gruss, P. (1997) The Pax4 gene is essential for differentiation of insulin-producing β cells in the mammalian pancreas, *Nature 386*, 399−402.
12. Torres, M., Gomez-Pardo, E., Dressler, G. R., and Gruss, P. (1995) Pax-2 controls multiple steps of urogenital development, *Development 121*, 4057−4065.
13. Bober, E., Franz, T., Arnold, H. H., Gruss, P., and Tremblay, P. (1994) Pax-3 is required for the development of limb muscles: A possible role for the migration of dermomyotomal muscle progenitor cells, *Development 120*, 603−612.
14. Goulding, M. D., Chalepakis, G., Deutsch, U., Erselius, J. R., and Gruss, P. (1991) Pax-3, a novel murine DNA binding protein expressed during early neurogenesis, *EMBO J. 10*, 1135−1147.
15. Auerbach, R. (1954) Analysis of the developmental effects of a lethal mutation in the house mouse, *J. Exp. Zool. 127*, 305−329.
16. Baldwin, C. T., Hoth, C. F., Amos, J. A., da-Silva, E. O., and Milunsky, A. (1992) An exonic mutation in the HuP2 paired domain gene causes Waardenburg's syndrome, *Nature 355*, 637−638.
17. Baldwin, C. T., Hoth, C. F., Macina, R. A., and Milunsky, A. (1995) Mutations in PAX3 that cause Waardenburg syndrome type I: Ten new mutations and review of the literature, *Am. J. Med. Genet. 58*, 115−122.
18. Beechey, C. V., and Searle, A. G. (1986) Mutations at the Sp Locus, *Mouse News Lett. 75*, 28.
19. Franz, T. (1989) Persistent truncus arteriosus in the Splotch mutant mouse, *Anat. Embryol. 180*, 457−464.
20. Franz, T. (1990) Defective ensheathment of motoric nerves in the Splotch mutant mouse, *Acta Anat. 138*, 246−253.
21. Goulding, M., Lumsden, A., and Paquette, A. J. (1994) Regulation of Pax-3 expression in the dermomyotome and its role in muscle development, *Development 120*, 957−971.
22. Barr, F. G., Galili, N., Holick, J., Biegel, J. A., Rovera, G., and Emanuel, B. S. (1993) Rearrangement of the PAX3 paired box gene in the paediatric solid tumour alveolar rhabdomyosarcoma, *Nat. Genet. 3*, 113−117.
23. Galili, N., Davis, R. J., Fredericks, W. J., Mukhopadhyay, S., Rauscher, F. J., III, Emanuel, B. S., Rovera, G., and Barr, F. G. (1993) Fusion of a fork head domain gene to PAX3 in the solid tumour alveolar rhabdomyosarcoma, *Nat. Genet. 5*, 230−235.
24. Noll, M. (1993) Evolution and role of Pax genes, *Curr. Opin. Genet. Dev. 3*, 595−605.
25. Xu, H. E., Rould, M. A., Xu, W., Epstein, J. A., Maas, R. L., and Pabo, C. O. (1999) Crystal structure of the human Pax6 paired domain-DNA complex reveals specific roles for the linker region

and carboxy-terminal subdomain in DNA binding, *Genes Dev. 13*, 1263−1275.
26. Xu, W., Rould, M. A., Jun, S., Desplan, C., and Pabo, C. O. (1995) Crystal structure of a paired domain-DNA complex at 2.5 Å resolution reveals structural basis for Pax developmental mutations, *Cell 80*, 639−650.
27. Czerny, T., Schaffner, G., and Busslinger, M. (1993) DNA sequence recognition by Pax proteins: Bipartite structure of the paired domain and its binding site, *Genes Dev. 7*, 2048−2061.
28. Epstein, J., Cai, J., Glaser, T., Jepeal, L., and Maas, R. (1994) Identification of a Pax paired domain recognition sequence and evidence for DNA-dependent conformational changes, *J. Biol. Chem. 269*, 8355−8361.
29. Kappen, C., Schughart, K., and Ruddle, F. H. (1993) Early evolutionary origin of major homeodomain sequence classes, *Genomics 18*, 54−70.
30. Treisman, J., Gonczy, P., Vashishtha, M., Harris, E., and Desplan, C. (1989) A single amino acid can determine the DNA binding specificity of homeodomain proteins, *Cell 59*, 553−562.
31. Wilson, D., Sheng, G., Lecuit, T., Dostatni, N., and Desplan, C. (1993) Cooperative dimerization of paired class homeo domains on DNA, *Genes Dev. 7*, 2120−2134.
32. Wilson, D. S., Guenther, B., Desplan, C., and Kuriyan, J. (1995) High resolution crystal structure of a paired (Pax) class cooperative homeodomain dimer on DNA, *Cell 82*, 709−719.
33. Underhill, D. A., Vogan, K. J., and Gros, P. (1995) Analysis of the mouse Splotch-delayed mutation indicates that the Pax-3 paired domain can influence homeodomain DNA-binding activity, *Proc. Natl. Acad. Sci. U.S.A. 92*, 3692−3696.
34. Fortin, A. S., Underhill, D. A., and Gros, P. (1998) Helix 2 of the paired domain plays a key role in the regulation of DNA-binding by the Pax-3 homeodomain, *Nucleic Acids Res. 26*, 4574−4581.
35. Fortin, A. S., Underhill, D. A., and Gros, P. (1997) Reciprocal effect of Waardenburg syndrome mutations on DNA binding by the Pax-3 paired domain and homeodomain, *Hum. Mol. Genet. 6*, 1781−1790.
36. Apuzzo, S., and Gros, P. (2002) Site-specific modification of single cysteine Pax3 mutants reveals reciprocal regulation of DNA binding activity of the paired and homeo domain, *Biochemistry 41*, 12076−12085.
37. Apuzzo, S., Abdelhakim, A., Fortin, A. S., and Gros, P. (2004) Cross-talk between the paired domain and the homeodomain of Pax3: DNA binding by each domain causes a structural change in the other domain, supporting interdependence for DNA binding, *J. Biol. Chem. 279*, 33601−33612.
38. Apuzzo, S., and Gros, P. (2006) The paired domain of Pax3 contains a putative homeodomain interaction pocket defined by cysteine scanning mutagenesis, *Biochemistry 45*, 7154−7161.
39. Chalepakis, G., and Gruss, P. (1995) Identification of DNA recognition sequences for the Pax3 paired domain, *Gene 162*, 267−270.
40. Epstein, J. A., Lam, P., Jepeal, L., Maas, R. L., and Shapiro, D. N. (1995) Pax3 inhibits myogenic differentiation of cultured myoblast cells, *J. Biol. Chem. 270*, 11719−11722.
41. Jun, S., and Desplan, C. (1996) Cooperative interactions between paired domain and homeodomain, *Development 122*, 2639−2650.
42. Loo, T. W., and Clarke, D. M. (2001) Cross-linking of human multidrug resistance P-glycoprotein by the substrate, tris(2-maleimidoethyl)amine, is altered by ATP hydrolysis. Evidence for rotation of a transmembrane helix, *J. Biol. Chem. 276*, 31800−31805.
43. Tell, G., Scaloni, A., Pellizzari, L., Formisano, S., Pucillo, C., and Damante, G. (1998) Redox potential controls the structure and DNA binding activity of the paired domain, *J. Biol. Chem. 273*, 25062−25072.
44. Jabet, C., Gitti, R., Summers, M. F., and Wolberger, C. (1999) NMR studies of the pbx1 TALE homeodomain protein free in solution and bound to DNA: Proposal for a mechanism of HoxB1-Pbx1-DNA complex assembly, *J. Mol. Biol. 291*, 521−530.
45. Piper, D. E., Batchelor, A. H., Chang, C. P., Cleary, M. L., and Wolberger, C. (1999) Structure of a HoxB1-Pbx1 heterodimer bound to DNA: Role of the hexapeptide and a fourth homeodomain helix in complex formation, *Cell 96*, 587−597.
46. Sprules, T., Green, N., Featherstone, M., and Gehring, K. (2000) Conformational changes in the PBX homeodomain and C-terminal extension upon binding DNA and HOX-derived YPWM peptides, *Biochemistry 39*, 9943−9950.
47. Sprules, T., Green, N., Featherstone, M., and Gehring, K. (2003) Lock and key binding of the HOX YPWM peptide to the PBX homeodomain, *J. Biol. Chem. 278*, 1053−1058.
48. Qian, Y. Q., Resendez-Perez, D., Gehring, W. J., and Wuthrich, K. (1994) The des(1−6)antennapedia homeodomain: Comparison of the NMR solution structure and the DNA-binding affinity with the intact Antennapedia homeodomain, *Proc. Natl. Acad. Sci. U.S.A. 91*, 4091−4095.
49. Clarke, N. D., Kissinger, C. R., Desjarlais, J., Gilliland, G. L., and Pabo, C. O. (1994) Structural studies of the engrailed homeodomain, *Protein Sci. 3*, 1779−1787.
50. Cox, M., van Tilborg, P. J., de Laat, W., Boelens, R., van Leeuwen, H. C., van der Vliet, P. C., and Kaptein, R. (1995) Solution structure of the Oct-1 POU homeodomain determined by NMR and restrained molecular dynamics, *J. Biomol. NMR 6*, 23−32.
51. Green, N. S., Reisler, E., and Houk, K. N. (2001) Quantitative evaluation of the lengths of homobifunctional protein cross-linking reagents used as molecular rulers, *Protein Sci. 10*, 1293−1304.
52. Bendall, A. J., Ding, J., Hu, G., Shen, M. M., and Abate-Shen, C. (1999) Msx1 antagonizes the myogenic activity of Pax3 in migrating limb muscle precursors, *Development 126*, 4965−4976.

BI062107Q